Fonds Régional de Développement Européen
European Regional Development Fund

ICE
INTELLIGENT COMMUNITY ENERGY

Interreg
France (Channel Manche) England

EUROPEAN UNION

DELIVERABLE D222 APPLICATION OF THE TIDAL ENERGY AND WAVE ENERGY ASSESSMENT TOOLS TO THE ISLE OF PORTLAND

MARCH 2023

BRETAGNE DÉVELOPPEMENT INNOVATION
SDEF
TECHNOPÔLE BREST-IROISE
Technopole Quimper-Cornouaille
PÔLE MER
UNIVERSITY OF EXETER
PLYMOUTH UNIVERSITY
UEA University of East Anglia
marine

ICE report T2.2.2: Application of the Tidal Energy and Wave Energy Assessment Tool to the Isle of Portland

Jon Miles, Juliette Jackson

About ICE

Supported by Interreg VA France (Channel) England, the Intelligent Community Energy (ICE) project, aims to design and implement innovative smart energy solutions for isolated territories in the Channel area. Islands and isolated communities face unique energy challenges. Many islands have no connection to wider electricity distribution systems and are dependent on imported energy supplies, typically fossil fuel driven. The energy systems that isolated communities depend on tend to be less reliable, more expensive and have more associated greenhouse gas (GHG) emissions than mainland grid systems. In response to these problems, the ICE project considers the entire energy cycle, from production to consumption, and integrates new and established technologies in order to deliver innovative energy system solutions. The ICE consortium brings together researcher and business support organisations in France and the UK, and engagement with SMEs will support project rollout and promote European cooperation.

Part 1: Energy supply to the Isle of Portland using in-stream tidal energy.

Dr Jon Miles

Part 2: Energy supply to the Isle of Portland using wave energy.

Dr Juliette Jackson and Dr Jon Miles

Acknowledgements

Funding support for this work was received through the INTERREG France Channel England (FCE) European Commission Intelligent Community Energy (ICE) project.

Energy supply to the Isle of Portland using in-stream tidal energy.

Dr Jon Miles

Report for the ICE Project, January 2023.

Abstract

An option for island and isolated communities with strong tidal currents is to harvest energy using in-stream tidal turbines. The Isle of Portland (south UK) has a small community of 12,800 people. It is known to have strong tidal currents off the southern tip of the island, reaching 7 knots. Using UK Admiralty chart data from the site, a method for generating time series of flow velocity at the site is demonstrated, by calculating solar (S2), lunar (M2) fortnightly and residual current components. The power generation characteristics of an example tidal turbine (Sabella) are used to generate a time series of power production for a single turbine. The annual energy production of a single turbine is calculated as 1,183 MWh at the site. With assumptions about individual electricity consumption of 2,900 kWh per person per year (Ofgem, 2022), it is estimated that an array of 32 turbines would cover the population requirements, however solutions such as storage or alternative supply would be required for slack water periods.

Introduction

The Isle of Portland is an island off the South Coast of the UK, attached to the mainland by a short spit. The island is known to have strong tidal currents off Portland Bill, the southern tip of the island. This paper investigates the tidal power that could be gained from the currents off Portland Bill, and considers this in context of the energy needs of the people living on the island. To achieve this, an indication of the strength of the tidal currents at the sites is gained from UK Admiralty Charts. An example of a possible tidal turbine is considered, such that the power generation characteristics can be incorporated. A time series of flow velocities at the sites is modelled using principal lunar and solar constituents. The power output from an individual device is calculated. The number of turbines and the length of a fence of turbines sufficient to power the whole island is then estimated.

Tidal Currents

The general shape of the Isle of Portland is shown in Figure 1. For this paper, a site has been identified at Portland Bill, on the southern tip of the Island.

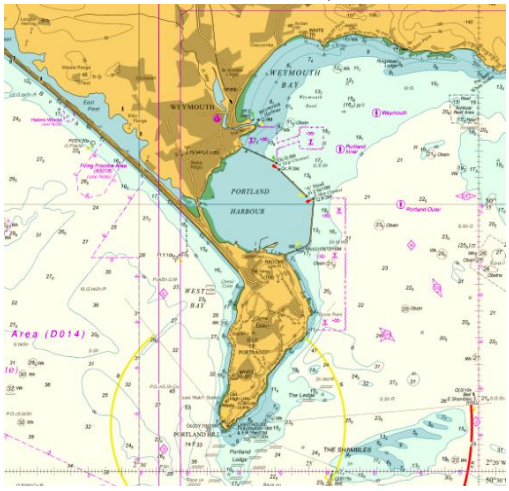

Figure 1: Cropped section of UK Admiralty Chart 2615 showing the Isle of Wight (not for Navigation). Reproduced for research purposes using Edina Digimap.

Figure 2 shows the bathymetry in more detail, indicating a tide race over the relatively shallow Portland Ledge (~10 m water depth). To the south of this, the water depth increases. A tidal diamond, where current speeds are known, is evident on the chart at location <T>, in approximately 30 m water depth. The depth of 30 m gives potential for a 10 m diameter turbine with 10 m clearance above and below, and is a similar depth to that used at Ramsey Sound by the Tidal Energy Limited (TEL) device.

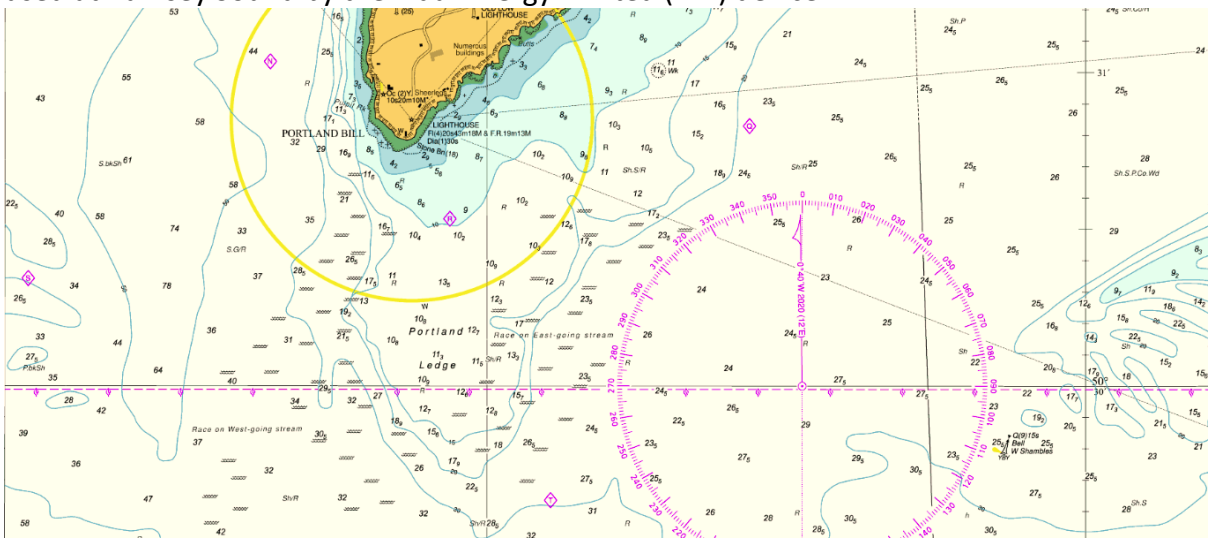

Figure 2: The southern tip of the Isle of Portland, showing tidal diamond <T> to the south-east of Portland Ledge. Reproduced for research purposes only using Edina Digimap, based on Admiralty Chart 2035 (not for Navigation).

The UK Admiralty charts indicate a variety of tidal diamonds in the general area. At the position of these diamonds, measurements have been made by the UK Admiralty of the

flow velocity during Spring tides and during Neap tides, during quiescent weather. Data for tidal diamond <T> are given in Figure 3. The tidal diamond data from the charts can be used to give the maximum flow rates at Spring and Neap tides, both for the flood and ebb tide, which allows subsequent modelling of the flow velocity time series. Such data have been used to verify the performance of high-resolution models of flow velocity (e.g. Haverson et al., 2018). The key data for Portland used in the analysis here are shown in Table 1. The maximum Spring tide flow rates at diamond T are 7.0 knots, and the maximum Neap tide rates reach 3.5 knots. Although there are other tidal diamonds in the general area, the analysis here is limited to <T> in the first instance. At spring tides, there is a difference between maximum Westerly directed flow (7.0 knots), and the maximum Easterly flow (5.6 knots), suggesting a residual. A smaller magnitude difference occurs at neaps, with the tide strengths of 3.5 knots (Westerly) and 2.8 knots (Easterly). A conversion from knots to m/s allows flows to be considered in standard units for power calculations.

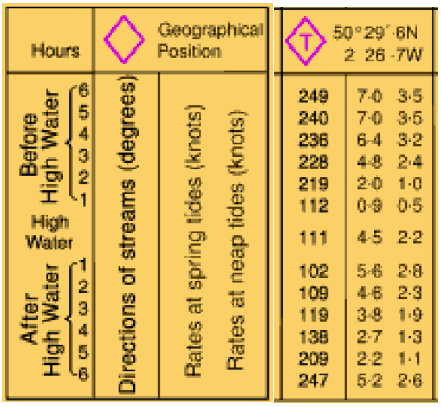

Figure 3. Tidal diamond data off Portland Bill at tidal diamond <T>. Reproduced for research purposes only using Edina Digimap, based on Admiralty Chart 2255 (not for Navigation). Times are relative to HW Plymouth (Devonport).

Table 1. Velocities at the site from the tidal diamond. Current flowing generally to the West or East is indicated by W and E, respectively.

	Knots	Time relative to Plymouth (Devonport)	Direction of flow (degrees)	General direction (relative to Channel)
Spring W	7.0	6 hrs before HW	249	W
Spring E	5.6	1 hr after HW	102	E
Neap W	3.5	6 hrs before HW	240	W
Neap E	2.8	1 hr after HW	102	E

The variation in flow strength through the tide, as indicated by the tidal diamond for Portland Bill is shown in Figure 4. To illustrate the directional variation, flows are assigned a positive or negative value, with flows heading generally to the West as positive, and those generally to the East as negative. The general form of the velocity variability is approximately sinusoidal, however the flows directed generally towards the East are generally larger than the flows to the West. Neap tide flows are by nature slower than the Spring tide flows.

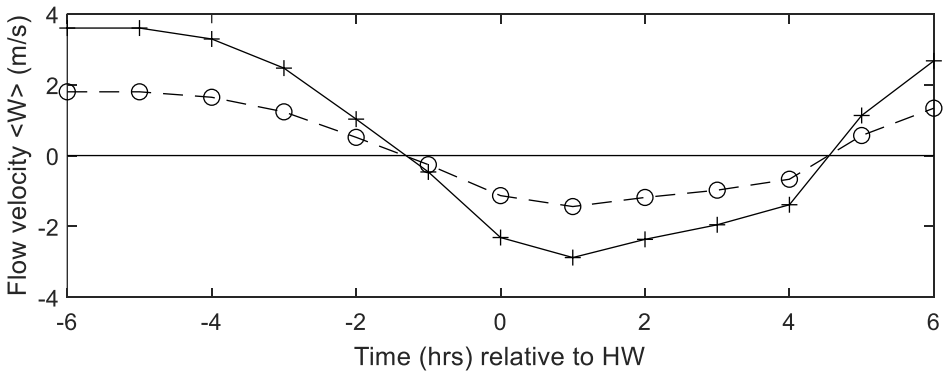

Figure 4. Plot of flow velocities, converted to m/s, at the location of Tidal Diamond T at Portland Bill. Neap tides are shown by the dashed lines, spring tides by the solid lines. Generally Westerly directed flows are assigned positive values. Times are relative to HW Portsmouth.

Tidal flow modelling

A prediction of the flow conditions at the sites can be made using the flow observations at the Tidal Diamonds. In order to achieve this, the lunar (M2), solar (S2), fortnightly (f14) and residual (R) contributions to the velocity need to be calculated at the position of the diamonds, using the tidal diamond data.

Tidal velocity calculation detail

The tidal variations can be decomposed from the observed flow velocities given at the tidal diamond using the spring and neap current speeds for the maximum flood and ebb flows. The method assumes that the flows are approximately rectilinear; i.e. the maximum in the flood direction is in the opposite direction to the maximum ebb. For the purpose of this illustration, the larger of the two is assumed to be the flood.

If the only variation in tidal current is due to lunar (M2) and solar (S2) constituents, it is possible to solve for the amplitudes of the velocity constituents. When maximum spring tides occur, the current due to the sun and moon may be considered to add together. The amplitude of the spring tide component may be considered as:

$$u_{spring} = u_{M2} + u_{S2}$$

When neap tides occur, the current due to the sun and moon may be considered to act against each other:

$$u_{neap} = u_{M2} - u_{S2}$$

Adding equations for u_{spring} and u_{neap} gives:

$$u_{M2} = \frac{u_{spring} + u_{neap}}{2}$$

Subtracting yields:

$$u_{S2} = \frac{u_{spring} - u_{neap}}{2}$$

However, in practice the data from the tidal diamond indicates that there is a residual (non-zero) mean current, and that this varies from springs to neaps. By assuming that the M2 and S2 components are oscillating relative to a steady residual current, and a fortnightly variation in this residual, it is possible to predict the time series of velocity from the tidal diamond data.

Tidal velocity amplitude

If is first necessary to identify the spring maximum in the flood direction (u_{sf}) and the maximum flow in the ebb direction (u_{se}) from the tidal diamond. It is also necessary to identify the neap tide maximum in the flood direction (u_{nf}) and the neap tide maximum flow in the ebb direction (u_{ne}).

A definition sketch for the series of calculations required is given in Figure 5.

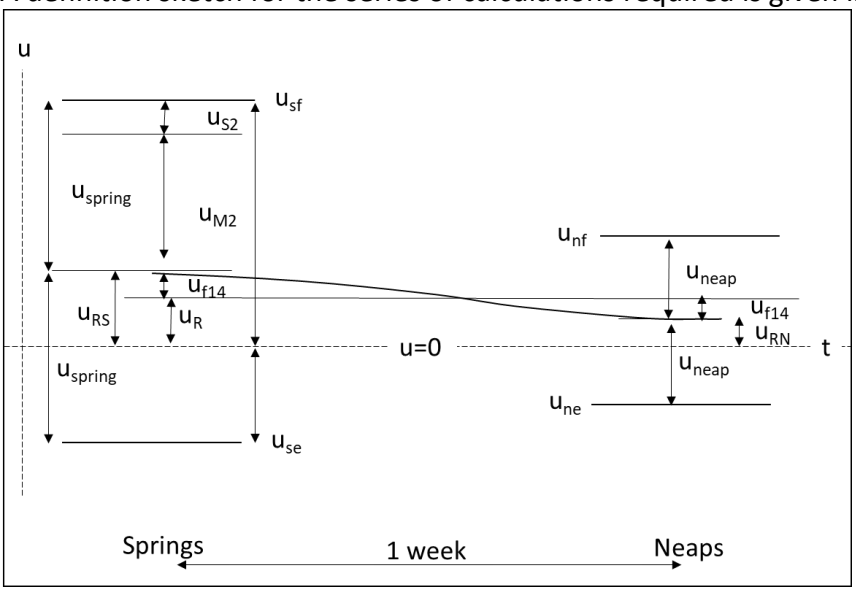

Figure 5. Sketch to illustrate the position of different contributing components to tidal velocity.

The amplitude of the spring tide and neap tide oscillations can be ascertained as follows:

$$u_{spring} = \frac{u_{sf} + u_{se}}{2}$$

$$u_{neap} = \frac{u_{nf} + u_{ne}}{2}$$

The residual current at springs (u_{RS}) and neaps (u_{RN}) is given by the difference in flood and ebb velocities:

$$u_{RS} = \frac{u_{sf} - u_{se}}{2}$$

$$u_{RN} = \frac{u_{nf} - u_{ne}}{2}$$

Assuming that the variations are driven primarily by lunar and solar components, and that the oscillations take place about the residual, the M2 and S2 amplitudes can be calculated as:

$$u_{M2} = \frac{u_{spring} + u_{neap}}{2}$$

$$u_{S2} = \frac{u_{spring} - u_{neap}}{2}$$

The variation in the residual between springs and neaps is assumed to be sinusoidal, and the amplitude of this oscillation is given by:

$$u_{f14} = \frac{u_{RS} - u_{RN}}{2}$$

The average residual for the spring neap cycle is assumed as constant, and is given by:

$$u_R = \frac{u_{RS} + u_{RN}}{2}$$

Frequencies

The time step in the creation of the velocity time series is assumed to be 1 hr. It is possible to assume that the period of the solar and lunar constituents are 12 and 12.42 hrs respectively, and achieve a satisfactory result.

Alternatively, a more accurate estimate over a year may be incorporated by using a tide table from the standard port (that the tidal diamond table refers to). Observations from the tide table of high spring tides that are temporally separated are needed (e.g. ~1 year apart). If the date and time of first of these observations is denoted t_1, and the second is denoted t_2, the time (in hours) between these spring tides can be calculated. The number of spring tides (n) needs to be identified within this time (i.e. how many 14 day cycles there are). The period of the spring tides (i.e. approximately 14 days) is therefore identifiable from the tide tables as:

$$T_{spring} = \frac{t_2 - t_1}{n}$$

The frequency of spring tides is given by:

$$f_{spring} = \frac{1}{T_{spring}}$$

The period of the solar component (T_{S2}) is 12 hrs, so the frequency is given by:

$$f_{S2} = \frac{1}{T_{S2}}$$

The frequency of the lunar component (f_{M2}) is given by:

$$f_{M2} = f_{S2} - f_{spring}$$

The period of the lunar component is:

$$T_{M2} = \frac{1}{f_{M2}}$$

The fortnightly component that quantifies the oscillation of the mean about the residual has a period that is the same as the springs:

$$T_{f14} = T_{spring}$$

The radial frequencies (ω) required for recreating the tidal time series are given by:

$$\omega_{S2} = \frac{2\pi}{T_{S2}}$$

$$\omega_{M2} = \frac{2\pi}{T_{M2}}$$

$$\omega_{f14} = \frac{2\pi}{T_{f14}}$$

The components are assumed to oscillate sinusoidally. In re-creating the time series, if the time series starts with the addition of M2 and S2 components, the time series starts with spring tides. The fortnightly variation in the residual is maximum at spring tides, and is therefore described using a cosine. This ensures that the peak in the f14 component is in phase with the spring tides.

The equation for the velocity (u) as a function of time (t) is given by:

$$u(t) = u_{M2}\sin(\omega_{M2}t) + u_{S2}\sin(\omega_{S2}t) + u_{f14}\cos(\omega_{f14}t) + u_R$$

M2 indicates the principal lunar constituent with a period of approximately 12.42 hrs, S2 indicates the principal solar constituent with a period of 12 hrs, f14 indicates a fortnightly variation, and R indicates a residual constant value. ω indicates the angular frequency (ω = 2 π/ f), f is frequency (f=1/T), and T is the period of oscillation. A time step of 1 hr is used here, however finer resolution time steps in generating velocity time series would be possible.

Tidal flow data generated for Portland Bill

The analysis above applied to Portland Bill tidal diamond T data gives an M2 amplitude u_{M2} of 3.1 knots, an S2 amplitude u_{S2} of 1.05 knots, a residual mean u_R of 0.2 knots, and a residual oscillation u_{f14} of 0.05 knots. An examination of the tide tables for the nearby port of Plymouth indicates 23 spring tides in 338.967 days, giving a spring tide period (T_{spring}) of 353.705 hrs. The solar period (T_{S2}) is 12 hrs, and the lunar period (T_{M2}) is therefore 12.4214 hrs.

A plot of the time series generated for Portland Bill at tidal diamond T is shown in Figure 6. The data from the tidal diamonds are overlaid.

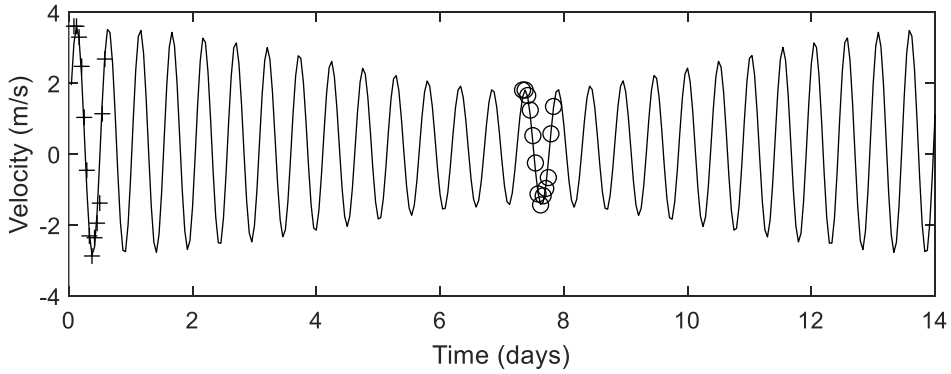

Figure 6. Time series of flow velocities (m/s) varying with time (days) at Portland Bill predicted using Tidal Diamond <T> from Admiralty Chart 2255. Also marked are the tidal diamond data from the Tidal Diamond for Spring tides (+) and Neap tides (x), converted to m/s.

The time series of velocity allows a time series of power generation by a tidal turbine to be calculated.

Tidal Turbine

In-stream tidal turbines are essentially submerged equivalents to wind turbines, but placed either on the sea floor, or positioned below a floating vessel. Figure 7 shows the Sabella D10, which is considered conceptually in the analysis below (Sabella, n.d.). The Sabella D-10 is a 10 meter diameter turbine that rotates at 5 to 20 revolutions per minute, with a maximum power output of 1 MW in 4 m/s of flow. (Sabella, n.d.; Lewis et al., 2021). The structure is 17 m high, weights 450 tons, and has a footprint that is 20 m x 20 m. The device has been deployed successfully off the Islands of Ushant in Brittany (France). Sabella have subsequently been developing the D-15, which is a 15 m diameter version with increased power output of 2.3 MW.

Figure 7. Sabella D-10 In-stream tidal turbine.

Power production by In-stream tidal turbines

The use of the predicted time series of velocity data allows an estimate of tidal power at the site. The power available from the tidal stream is given by Lewis et al (2021) and many authors previously as:

$$P = \frac{1}{2}\rho C_p A u^3$$

where P has units of Watts, ρ is the density of seawater (taken here as 1025 kg/m^3). C_p is a turbine coefficient that identifies the efficiency of the turbine, A is the swept area of the turbine, and u is the flow speed (units of m/s).

The swept area depends on the diameter (D) of the turbine as:

$$A = \frac{\pi D^2}{4}$$

If considering the fluid power alone, it would be possible to use a value of $C_p = 1$. However, turbines are not able to convert all the fluid power to electrical power, so a value of $C_p < 1$ is required. A standardised approach to identifying the turbine coefficient, based on a range of operational turbines, was put forward by Lewis et al (2021).

Turbines have a 'rated power' (P_r), which is the maximum power that they will generate, regardless of how much the flow increases. When the rated power is achieved at the lowest possible velocity, this is defined as the rated velocity (u_r). Turbines also generally have a 'cut in' speed, which identifies the flow velocity at which they start generating electricity (u_s). This may be expressed as a proportion of the rated velocity, i.e.

$$u_c = ku_r$$

For a general 'average' turbine, Lewis et al. (2021) gave k = 0.3, giving an average cut in speed as $u_s = 0.3\ u_r$. An average value of C_p was determined for a range of turbines as 0.37. Specific values some of the different turbines are given by Lewis et al (2021).
The power generation, in gradually increasing flow speeds, is defined as follows:
when $u < u_c$

$$P = 0$$

when $u_c < u < u_r$

$$P = \frac{1}{2}\rho C_p A u^3$$

when $u > u_r$

$$P = \frac{1}{2}\rho C_p A u_r^3$$

Values for the two Sabella Turbines and an 'average' set of values are given in Table 2. Further examples are given in Lewis et al (2021).

Table 2: Characteristic values of example and average turbines (adapted from Lewis et al., 2021)

	D (m)	P_r (kW)	u_r (m/s)	u_s (m/s)	k (=u_r/u_s)	C_p	Source
Sabella D-15	15	2300	4	1	0.25	0.4	Sabella website: Sabella published turbine characteristics. https://www.sabella.bzh/ en, 2019
Sabella D-10	10	1000	4	1	0.25	0.4	Sabella website: Sabella published turbine characteristics. https://www.sabella.bzh/ en, 2019
Average of 14 different turbines	13	816	2.91	0.88	0.30	0.37	Lewis et al (2021)

Power modelling

Starting with the tidal flow time series, the tidal power can be calculated, using a representative turbine (Sabella D-10). Figure 8 shows the tidal flow speed and the tidal power generated for a 1 week period at Portland, leading from Springs to Neaps. The horizontal lines in the top plot indicate the cut in speed used in the analysis. The power generated is shown in the lower plot.

Production is 0 kW when the tide is turning or when the flow is less than turbine cut in speed. Peak power production at maximum spring flow with one turbine is 750 kW (0.75

MW). The average power production including times of no generation is 135 kW. With 8,760 hrs in a year, the turbine gives an annual production of approximately 1,183 MWh.

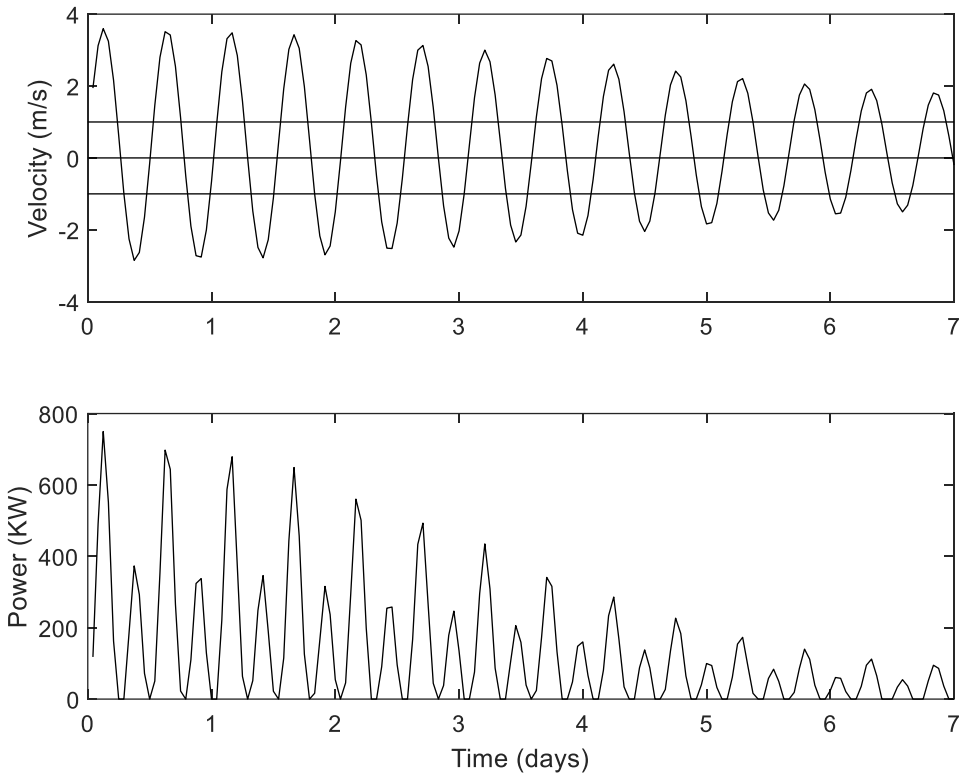

Figure 8. Power production potential at Portland from a single Sabella D10 device over a spring-neap period of 1 week.

Application in relation to Portland power requirements

In order to scale up the power production towards meeting island energy demands, it is clear that more than one turbine would be required. Conceptually, a fence of turbines across the flow is considered here, and the length of the fence is calculated to meet annual demand. It is assumed that a shore based power storage system or a cable linking in the Portland system with that of mainland UK would be in place to deal with the problem of smoothing out the daily and weekly variations. To reduce the length of the fence line as far as possible, while minimising wake effects, the turbines are conceptually considered to be placed in two parallel lines, with one diameter spacing between turbines in the front row, and further turbines located in the spaces between turbines, a small distance downstream. The required fence length value presented is therefore (approximately) a direct multiple of the number of turbines required and the turbine diameter.

One way to quantify the required tidal contribution is to consider the energy requirements of the Island for a year. The population of Portland is approximately 12,797 people. In the UK, the average consumption of electrical energy per person per year is approximately 2,900 kWh yr^{-1}. The Isle of Portland would currently therefore need 37,111,300 kWh, or 37,111 MWh per year.

Given the annual turbine power output for a single turbine, it is possible to calculate the length of a fence of turbines that would be needed to generate sufficient power for the island. For Portland Bill to generate the 37,111 MWh using turbines each generating 1,183 MWh requires 32 turbines. The line of turbines would need to stretch over a length of 320 m (Table 3).

Table 3: Energy demand and generation by tidal turbines

	Portland Bill
Annual Island demand	37,111 MWh
Annual turbine power production (single 10m diameter turbine)	1,183 MWh
Number of Turbines required to meet demand	32
Fence Length	320 m

While the array approach could include two rows of turbines, other array shapes are possible, and optimisation may be beneficial to minimise wake interactions with devices downstream (Coles et al., 2020).

Discussion

Tidal flows off headlands and in channels offer a reliable source of marine energy. In an island community, this energy source can usefully contribute to the overall energy mix, helping to provide a regular top up to a local grid (Coles et al., 2020). Ideally, the final planning of the installation of tidal energy devices would use Acoustic Doppler Current Profiler (ADCP) data from the site, combined with detailed numerical modelling, to characterise the resource precisely and deal with the spatial variations in velocity (e.g. Haverson et al., 2018). One of the difficulties in initial planning and conceptual modelling is that ADCP data may not be available, and it is expensive to gather this sort of data.

Furthermore, detailed three dimensional models are time consuming to implement and difficult to calibrate when there is no data from the site. The use of tidal diamonds from Admiralty Charts or current values from tidal atlas data helps to get round this problem for those interested in considering and quantifying the opportunities from the resource. The method is applicable as a first approximation, and is particularly well suited to those who have technical capability with programmes such as Excel and Matlab, but do not necessarily have background in detailed oceanographic modelling using packages such as Delft3D, Mike21 or Telemac.

The method includes M2 and S2 constituents, and the fortnightly variation in the residual. The method assumes a sinusoidal time series, and does not include the asymmetry or skewness in the velocity time series. This may be possible to some extent using the tidal diamond data, but requires further analysis beyond that offered here. The method does not include the monthly variation in Springs and Neaps (i.e. one neap or Spring tide is usually larger than the next one). It also does not include the seasonal variations in Springs and

Neaps, that lead to the largest tidal currents at the equinox. These longer oscillations are not included in tidal diamond data, and to include these things would require in-depth analysis of long time series of ADCP data. However, the M2 and S2 constituents are known to be the two major components, and the fundamental drivers of tidal currents. Other effects such as wind and waves may also affect the strength of the current on a particular day (e.g. Hardwick et al., 2021).

This study offers a conceptual view of the use of tidal currents to power the electricity needs of the Isle of Portland. It does not consider issues such as the cost of deployments, the consenting issues, wildlife, shipping, or the history or politics of tidal energy at the sites, or the alternative source of energy. However, the power generation values may be of interest to developers considering using the site.

Further detailed flow modelling of the area is possible, to look at different sites and local variations in flow velocity away from the tidal diamonds. Different turbines are possible, and these may yield different power output, depending on their cut in speed and their rating. Clearly these would be optimised for such a deployment. Although the length of fence of turbines identified meets the Island energy needs overall, the power production varies with time, and goes to zero when the current is slack. Tidal turbines would therefore need to be balanced by a suitable energy storage method, supply from a different source, or a cable to the mainland grid.

The turbine chosen in this study (Sabella) is just one example of a turbine, but other turbines are possible. The diameter of the rotor in this example was 10 m, and other turbines have different diameters. Sufficient depth is needed above and below the turbine for marine life to pass by, and for vessels to pass. The effect of waves on turbines is not considered here, and the impacts of extreme storms, surges, or their impact on cables or deployment and maintenance are not considered.

Despite these shortcomings, the approach gives a good indication that the energy requirements for the Island of Portland can be met using tidal currents, as a significant part of the energy mix.

Conclusions

The Isle of Portland (south UK) has a small community of 12,800 people, and has strong tidal currents off the southern tip of the island, reaching 7 knots. Using UK Admiralty chart data from the site, a method for generating time series of flow velocity at the site was demonstrated, and the solar (S2), lunar (M2) fortnightly and residual current components were calculated. The power generation characteristics of an example tidal turbine (Sabella) were used to generate a time series of power production for a single turbine. The annual energy production of a single turbine was calculated as 1,183 MWh at the site. Assuming individual electrical consumption of 2,900 kWh per person per year, an array of 32 turbines was shown to be cover the population requirements, however solutions such as storage or alternative supply would be required for slack water periods.

References.

Coles, D.S., Angeloudis, A., Goss, Z., Miles, J., 2021. Tidal stream vs. wind energy: The value of cyclic power when combined with short-term storage in hybrid systems, Energies, 14:1106

Coles, D., Blunden, L., Bahaj, A., 2017. Assessment of the energy extraction potential at tidal sites around the Channel Islands. Energy 124, 171–186. (doi:10.1016/j.energy.2017.02.023)

Coles, D.S., Blunden, L.S., Bahaj, A.S., 2020. The energy yield potential of a large tidal stream turbine array in the Alderney Race: energy yield estimate for Alderney Race. Phil. Trans. R. Soc. A 378, 20190502. (doi:10.1098/rsta.2019.0502)

Hardwick, J., Mackay, E.B.L., Ashton, I.G.C., Smith, H.C.M., Thies, P.R., 2021. Quantifying the Effects of Wave—Current Interactions on Tidal Energy Resource at Sites in the English Channel Using Coupled Numerical Simulations. Energies, 14, 3625. https://doi.org/10.3390/en14123625

Haverson, D., Bacon, J., Smith, H.C., Venugopal, V., Xiao, Q., 2018. Modelling the hydrodynamic and morphological impacts of a tidal stream development in Ramsey Sound. Renew. Energy 126, 876–887. (doi:10.1016/j.renene.2018.03.084)

Lewis, M., O'Hara Murray, R., Fredriksson, S., Maskell, J., de Fockert, A., Neill, S., Robins, P., 2021. A standardised tidal-stream power curve, optimised for the global resource, Renewable Energy, vol. 170, pp. 1308-1323. https://doi.org/10.1016/j.renene.2021.02.032

Sabella website: Sabella published turbine characteristics. https://www.sabella.bzh/ en, 2019

Sabella. Ushant showcase of tidal energy worldwide. Sabella document. https://www.sabella.bzh/sites/default/files/upload/plaquettes/leaflet_d10_-_12_pages.pdf

Energy supply to the Isle of Portland using wave energy

Dr Juliette Jackson and Dr Jon Miles

Report for the ICE Project, January 2023.

Abstract

This case study is intended to inform a wider assessment and strategy on how wave energy can be utilised alongside multiple sources of renewable energy, such as wind, solar and tidal to support isolated and or island communities to establish optimal energy solutions and in becoming energy independent. A demonstration calculation is presented for the Isle of Portland on the South coast of the UK using a source of accessible local wave energy data for use in simple wave power calculations, recorded by a wave buoy located at nearby Chesil Beach. This study incorporates a full year of analysis and a comparison of energy available from winter (January) and summer (June) using data from five consecutive years. Hypothetical suggestions are presented that are based on an example device specification and on the results of full-scale energy device trials. The power generation characteristics of a caisson mounted oscillating water column are used to ascertain what size wave plant would be needed to fulfil the energy requirement of Portland given the potential wave power of the site. Usage by the local community allows an indicative calculation of the scale of the theoretical setup needed to provide adequate power. To meet the energy demand of the Isle of Portland with wave energy a structure of approximately 2400 m in length would be required.

Introduction

Steady progress is being made in technological developments in the marine renewable sector across the globe, and recent enthusiasm and necessity is likely to drive an increased rate of progress in the coming years as the climate emergency is realised, carbon emission targets are set and efforts to become increasingly sustainable are made.
A case-study is presented here, following the methodology of the ICE project Tool for Rapid Assessment of Wave Energy at Isolated Community Sites, and presenting demonstration calculations based on the Isle of Portland on the South coast of the UK. The calculations used wave data from the National Network of Regional Coastal Monitoring Programmes (NNRCMP, 2022), incorporating a full year of analysis and a comparison of energy available from winter (January) and summer (June) using data from five consecutive years to make rudimentary estimations of the scale of the wave device development needed to provide adequate power to the local community. Information about the power generation characteristics of an example wave turbine and power usage by the local community is fed into the assessment.
Portland is a small peninsula, 6 km long by 2.7 km wide, that extends from the coast of Dorset into the English Channel. Connected by the mainland only by a thin strip of land

(Chesil Beach), the area is frequently subjected to wave action and the prevailing wind direction is from the South West.

A variety of wave energy devices using different fundamental principles have been developed over recent years. For this case study a caisson based Oscillating Water Column (OWC) was selected as a representative device for the Isle of Portland, using the installation at Mutriku in Northern Spain as a model (Power Technology, 2021). The caisson based OWC has several practical benefits for island deployment. Firstly, the construction of concrete caissons for breakwaters is well practiced in port and harbour engineering settings.

Secondly, caisson OWCs have been demonstrated working at full scale, both at Mutriku and in Scotland (Limpet, Boake et al., 2002). Thirdly, the ability to access and maintain the turbines, and the ability to cable the power away from the devices all avoid the need for difficult marine operations with these devices. Compared to other devices, the OWC in modular concrete-based caissons are a low-cost, corrosion-resistant and low-maintenance option (Falcão, 2010).

An Oscillating Wave Convertor (OWC) is composed of a chamber containing a water column in its lower part with a submerged orifice, and an air pocket in its upper part. The air pocket is connected to the atmosphere via a small duct hosting a self-rectifying turbine. The device performance is enhanced when a U-shaped entrance is incorporated in the orifice. The working principle of the system is that with the action of the incident waves, the water inside the U-shaped duct is subject to a reciprocating motion (Figure 1). This motion induces alternately a compression and an expansion of the air pocket, which generates an air flow in the air duct. A turbine coupled to an electrical generator, installed into the air duct, is driven in this way to produce electrical energy (Wavenergy.It, 2014).

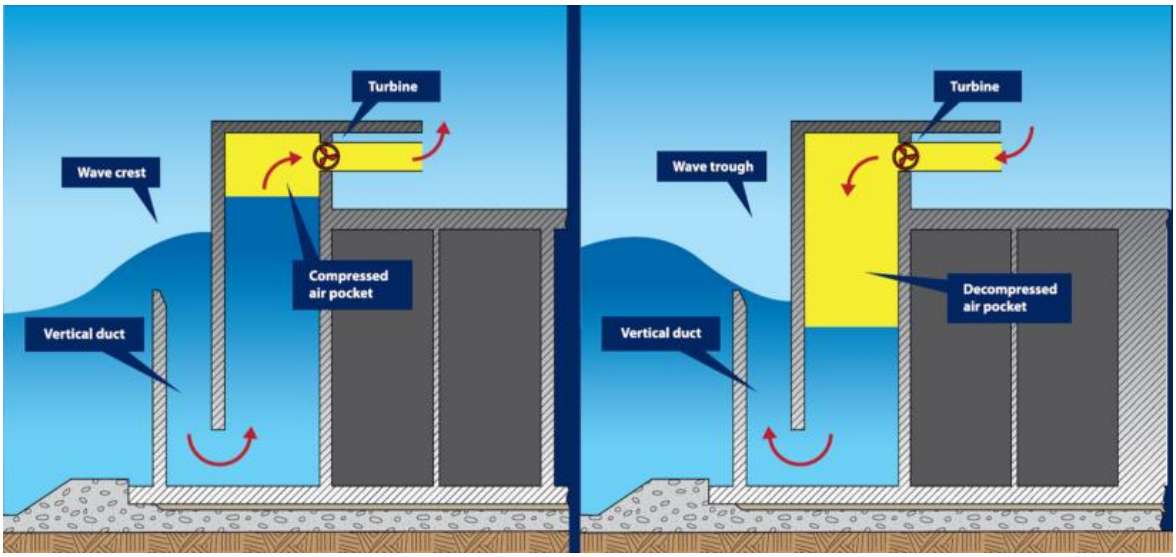

Figure 1: Oscillating water column concept diagram. (Wavenergy.It, 2014)

In Mutriku a detached, rubble mound breakwater of 440 m length was proposed to stop storm damage to the harbour, its piers and provide safe anchorage for boats. As a secondary function to coastal protection, several designs of Wave Energy Converters (WEC)

were considered for inclusion in the construction project (Power-technology, 2021). The Mutriku wave energy plant was commissioned in July 2011, built on a 100 m section of outer wall of the new breakwater. There are 16 air chambers, each 4.5 m wide and 3.1 m long, positioned 9.7 m above mean low water springs (MLWS) (BiMEP). Within each air chamber is a Wells turbine, a low-pressure air turbine that rotates continuously in one direction independent of the direction of the air flow, with the dimensions 2.83 m height, 1.25 m width and weighing 1200 kg. The turbines do not have a gearbox, hydraulics or pitching blades. The turbines are connected to a turbo generator with a capacity of 18.5 kW. The Mutriku plant generates an output of 295 kW, enough to power 250 households. (The average Spanish consumer uses around 10,500 kilowatt-hours (kWh) of electricity per year (IDAE 2011). This equates to an annual average rate of power use of 1.198 kW. Dividing the generated output of the Mutriku plant by the use figure gives the number of households powered: 295/1.198 = 247). This reduces carbon emissions annually by 600 t (Power-technology, 2021).

In addition to device development and full-scale deployment and trials, research continues to make progress in optimising plant design, increasing the energy harvest and increasing the energy density of waves. For example, introducing a 'zone-plate lens' changes the direction of wave propagation, so that incident water waves can be converged at a certain focal area (Stamnes, 1986).

A device will have an efficiency in generating electrical power from the available wave power. This efficiency depends on the wave height and period, and is defined by a power matrix. An estimation of the electricity production of a WEC in a specific site can be achieved by associating the power matrices of each WEC to the matrices that give the wave activity for the respective location in a determined time interval (Silva et al., 2013). The Power Matrix for the Mutriku plant isn't accessible, therefore the power matrix for the Oyster is given as it is a representative example for this case (Silva et al., 2013). The Oyster is an Oscillating Wave Surge Convertor that is a design progression from the LIMPET and suited for the shoreline or near shore environment (Folley et al., 2004).

Table 1: An example Power Matrix for the WEC, the Oyster (Silva et al., 2013).

	Oyster Power matrix (in kW)								
Te (s) *Hs (m)*	**5**	**6**	**7**	**8**	**9**	**10**	**11**	**12**	**13**
0.5	0	0	0	0	0	0	1	3	3
1	20	30	38	42	44	44	43	47	45
1.5	80	85	92	97	102	103	104	100	104
2	140	147	152	158	155	155	160	161	156
2.5	192	197	208	202	203	209	211	201	204
3	241	237	237	241	243	230	236	231	235
3.5	0	271	272	269	268	267	270	260	260
4	0	291	290	290	280	287	276	278	277
4.5	0	291	290	290	280	287	276	278	277
5	0	0	290	290	280	287	276	278	277
5.5	0	0	290	290	280	287	276	278	277
6	0	0	290	290	280	287	276	278	277

The power matrix indicates the energy output from a device for wave periods in the range 5 to 13 s, (columns) and wave heights in the range of 0.5 m to 6 m (rows). Energy units are in kW. The data here is for the Oyster device (Silva et al., 2013).

The device capture width (C_W) of the Oyster is 18 m (Whittaker). The power per m width of device (i.e. kW/m) can be calculated from:

$$P_{out}\ (kW/m) = \frac{P\ (kW)}{C_W}$$

This is illustrated for Oyster in Table 2.

Table 2: Power per m of wave front.

	Oyster Power matrix (in kW/m)								
Te (s) *Hs (m)*	**5**	**6**	**7**	**8**	**9**	**10**	**11**	**12**	**13**
0.5	0.00	0.00	0.00	0.00	0.00	0.00	0.06	0.17	0.17
1	1.11	1.67	2.11	2.33	2.44	2.44	2.39	2.61	2.50
1.5	4.44	4.72	5.11	5.39	5.67	5.72	5.78	5.56	5.78
2	7.78	8.17	8.44	8.78	8.61	8.61	8.89	8.94	8.67
2.5	10.67	10.94	11.56	11.22	11.28	11.61	11.72	11.17	11.33
3	13.39	13.17	13.17	13.39	13.50	12.78	13.11	12.83	13.06
3.5	0.00	15.06	15.11	14.94	14.89	14.83	15.00	14.44	14.44
4	0.00	16.17	16.11	16.11	15.56	15.94	15.33	15.44	15.39
4.5	0.00	16.17	16.11	16.11	15.56	15.94	15.33	15.44	15.39
5	0.00	0.00	16.11	16.11	15.56	15.94	15.33	15.44	15.39
5.5	0.00	0.00	16.11	16.11	15.56	15.94	15.33	15.44	15.39
6	0.00	0.00	16.11	16.11	15.56	15.94	15.33	15.44	15.39

The energy output from the Oyster is greatest at wave heights greater than 3.5 m and with wave periods of 6 s, with a slight decrease in energy output as the wave period increases.

Wave buoy data

The website for the National Network of Regional Coastal Monitoring Programmes (NNRCMP, 2022) of England acts as a single repository for coastal monitoring data collected by 6 regional programmes and aims to support coastal engineering and management. Combined data are freely accessible from the repository via the website and can be downloaded in yearly or monthly increments (NNRCMP, 2022). Other networks are accessible in different regions and countries.

The Centre for Studies and Expertise on Risks, the Environment, Mobility and Urban Planning (CEREMA) is the French major public agency for developing and capitalising on public expertise, including energy transition. CEREMA has been managing the national Centre d'Archiving National de Données de Houle InSitu (CANDHIS network) of wave

measuring stations along the French coast since 1972 although the site is under maintenance at the time of writing (CANDHIS, 2022).

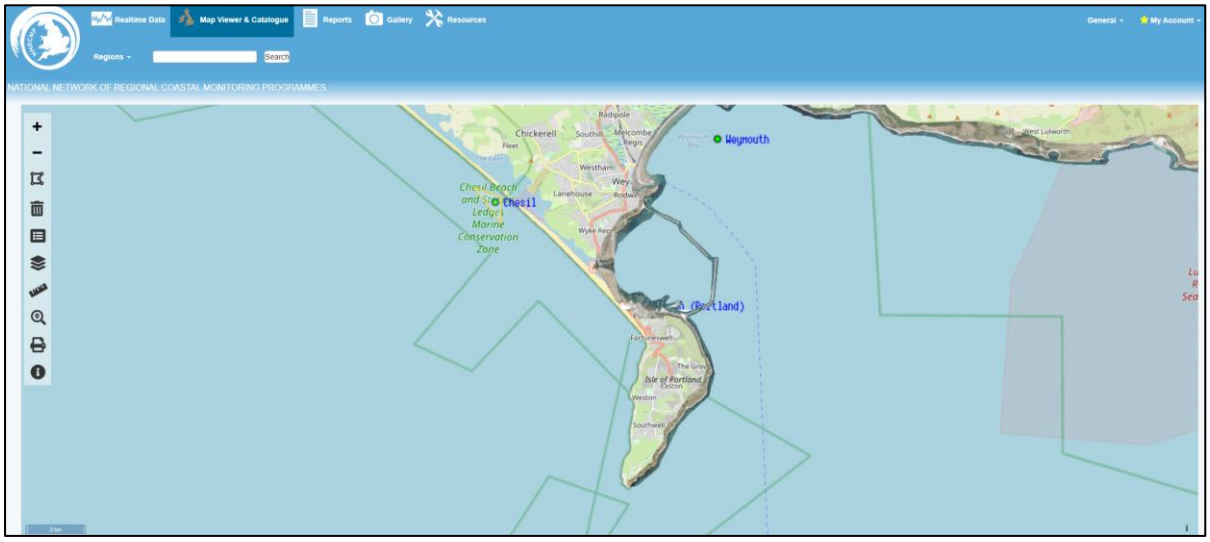

Figure 2: The National Network of Regional Coastal Monitoring Programme (NNRCMP) showing the location of the wave buoy at Chesil beach to the northwest of Portland (NNRCMP, 2022).

In this case, the NNRCMP collects data from its deployed Datawell directional Waverider buoys, plus data from 3 industry buoys provided by RWE Innogy and Wave Hub Limited. There are 13 Directional WaveRider buoys around the Southwest coast, each situated in ~10-12 m water depth (Chart Datum). The data is routed back to the National Coastal Monitoring Network website where it can be viewed in real-time, along with the data from the wave buoys in other regions. The real-time data isn't quality checked but archived data is retrospectively quality controlled and any errors with directional or wave height measurements are flagged, allowing wave data to be filtered and erroneous data points removed during data processing. The Waverider buoys record wave height, wave direction, direct pitch and roll. Data is recorded at 30 minute intervals. The buoys combine a horizontal accelerometer and a compass, enabling accurate and reliable directional wave data to be recorded. The resolution and accuracy of the heave range of the device is -20 m to +20 m, with a resolution of 0.01 m. The accuracy is < 0.5% of measured value after calibration, or < 1.0% of measured value after three years. The measurable wave period range is: 1.6 s - 30 s [5].

Figure 3: Waverider buoy (NNRCMP, 2022).

The wave buoy at Chesil, owned by Teignbridge District Council, was deployed on 22 December 2006. It is a Directional Waverider Mk111 Buoy, located OS 363094 E 78173 N; WGS84 Latitude: 50° 36.13' N Longitude: 02° 31.37' W (Figure 2). The wave buoy data is a source of readily accessible data from a variety of different platforms/websites. Each platform will process the raw data to their own specification and can be accessed from, two such sources are described here, the National Network of Regional Coastal Monitoring Programmes (NNRCMP, 2022) and the Centre for Environment, Fisheries and Aquaculture Science (CEFAS, 2022).

Wave statistics

To calculate wave power, the parameters significant wave height (H_s or Hm_0) and dominant (peak) wave period were selected for the time period of interest. For this initial study into the contribution of wave energy to the energy generation matrix of Portland, a year of recent data (2021) has been selected, and data for January and June for five different years has been downloaded for a winter-summer comparison.

Data imported into Microsoft Excel was plotted to reveal basic information about the wave conditions of a site. Wave height and period data for Chesil beach (Portland) is given in Figure 4. This shows that during 2021 there were multiple occurences of recorded wave heights in excess of 4 m, and wave periods of up to 25 s. However much of the time, wave heights are in the region of 0-1 m, with periods in the region 4-15 s. The average wave height for this year was 0.85 m and the average period was just over 8 s.

Plotting significant wave height against peak wave period helps to indicate outliers (Figure 5). Of the 1488 data points represented in Figure 5, the occurances where the wave period is between 5 and 7 seconds is the greatest, followed by occurances where the wave period is between 7 and 13 seconds. Few outliers show for January, with the most distinct being 1 meter wave height at 22 second wave period and four occurences of waves around 4 m in height and 15 – 20 seconds apart.

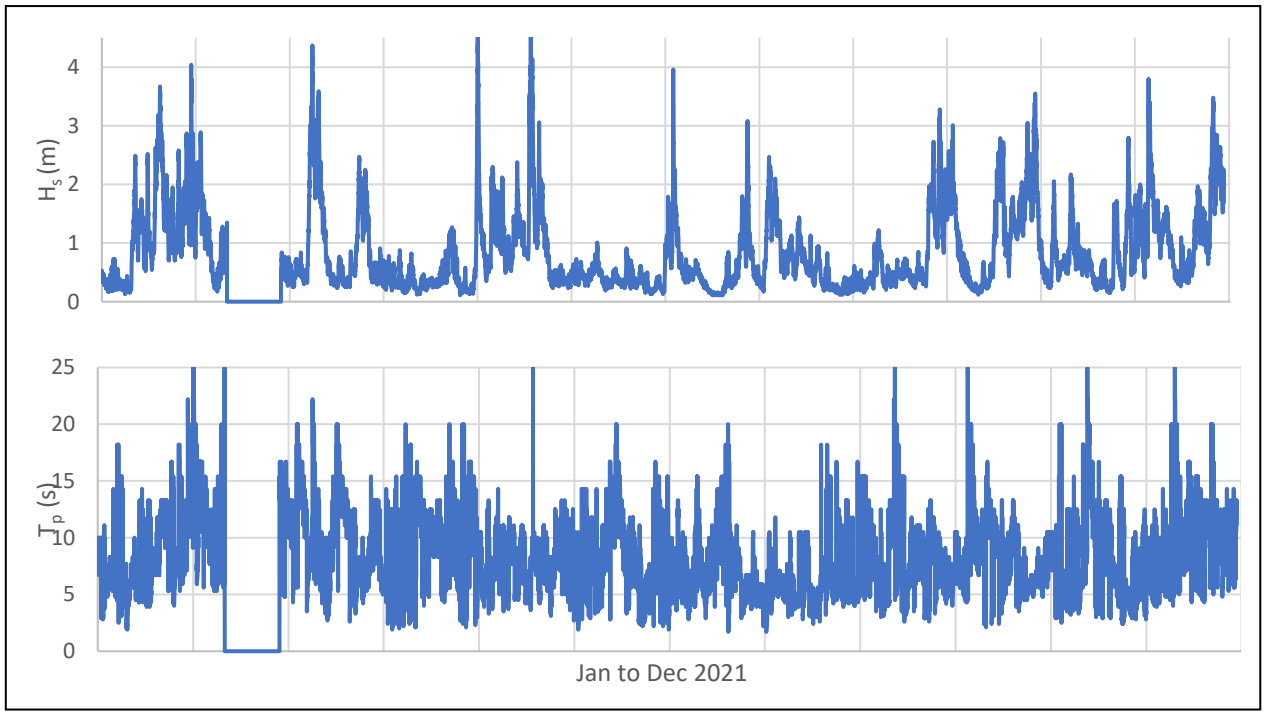

Figure 4: Significant wave height (H_S) and peak wave period (T_P) at the Chesil wave buoy, near Portland throughout 2021.

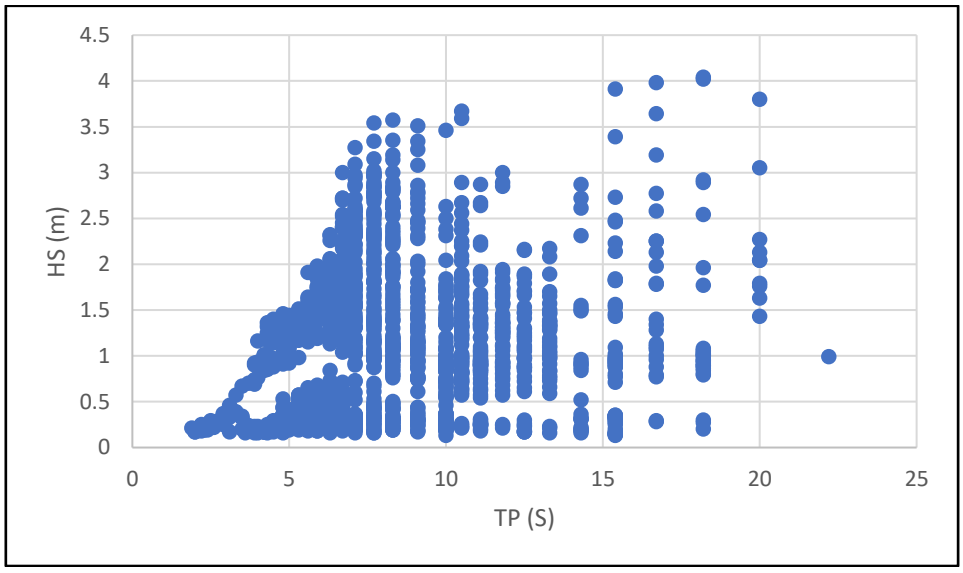

Figure 5: Significant wave height and peak wave period at the Chesil wave buoy, near Portland throughout January 2021.

It is worth noting that if data is missing from one repository, as in Figure 4 where some of the data from February is missing, it is possible that an alternative data repository for the required timeframe can be found, albeit possibly recorded at a different sensativity. The same data period has been accessed from the CEFAS repository (CEFAS, 2022, Figure 6) where all of the February data is present.

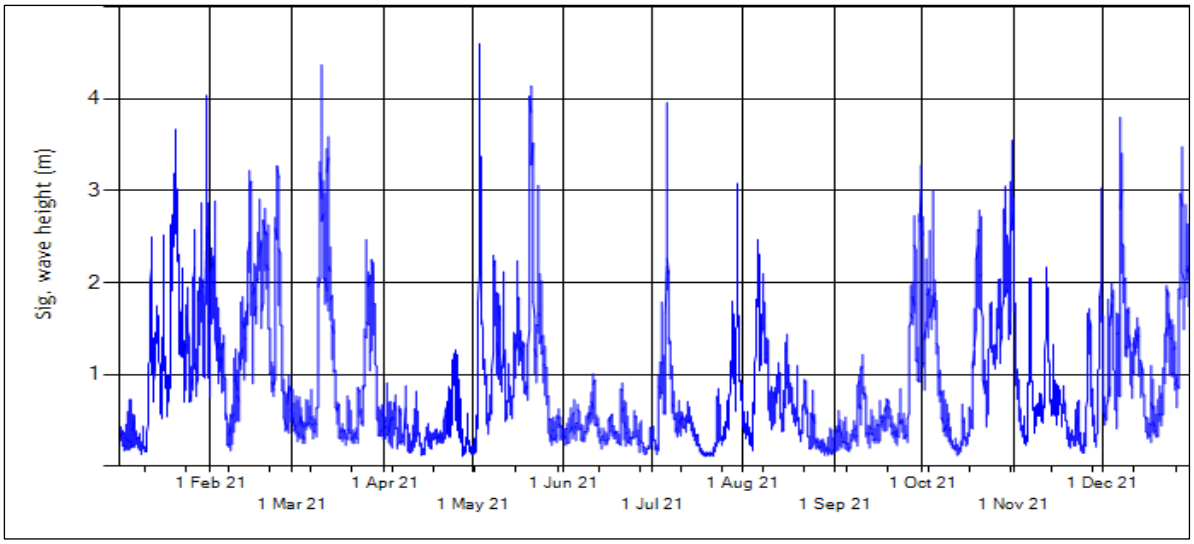

Figure 6: Significant wave height (H_S) at the Chesil wavebuoy, near Portland throughout 2021 (CEFAS 2022).

Calculating averages of wave heights over a suitable time period, such as daily averages, reduces the influence of winter storm conditions on the time series, and gives a picture of the seasonal variability in significant wave height and peak period between the winter and summer months. Understanding this variablilty over multiple years plays an important role in ensuring that assessments of power generation are realistic and meanigful.

The 2021 analyses suggested that January represented a winter 'stormy' period whilst June represented a summer 'calmer' period thus data for these two months were analysed for five separate years (Figure 7 and 8), this was particularly noticeable in 2018 and 2020. There was an unusually stormy period in early June 2017 with wave heights of almost 2.5 m. At the Chesil wave buoy, in January the average (instantaneous) significant wave height is 1.2 m, frequently exceeding 1 m throughout the year and exceeding 2 m on multiple occasions. In June the average significant wave height is 0.6 m and rarely exceeds 1 m (Figure 7). The average daily wave height for January is 1.6 m, while the average daily wave height for June is 0.6 m The average daily peak period in January is 9 seconds, within a range 3.5 to 16.7 seconds, while the average daily peak period for June is 7.5 seconds, and a range of 3.5 to 16.2. The wave period data indicates the contribution of both swell from distance storms with wave periods up to 15 seconds, and also locally generated wind seas with periods of 6 to 10 seconds (Figure 8). The summer data indicates periods of very low wave energy. This gives rise to some of the low values of wave period in the summer.

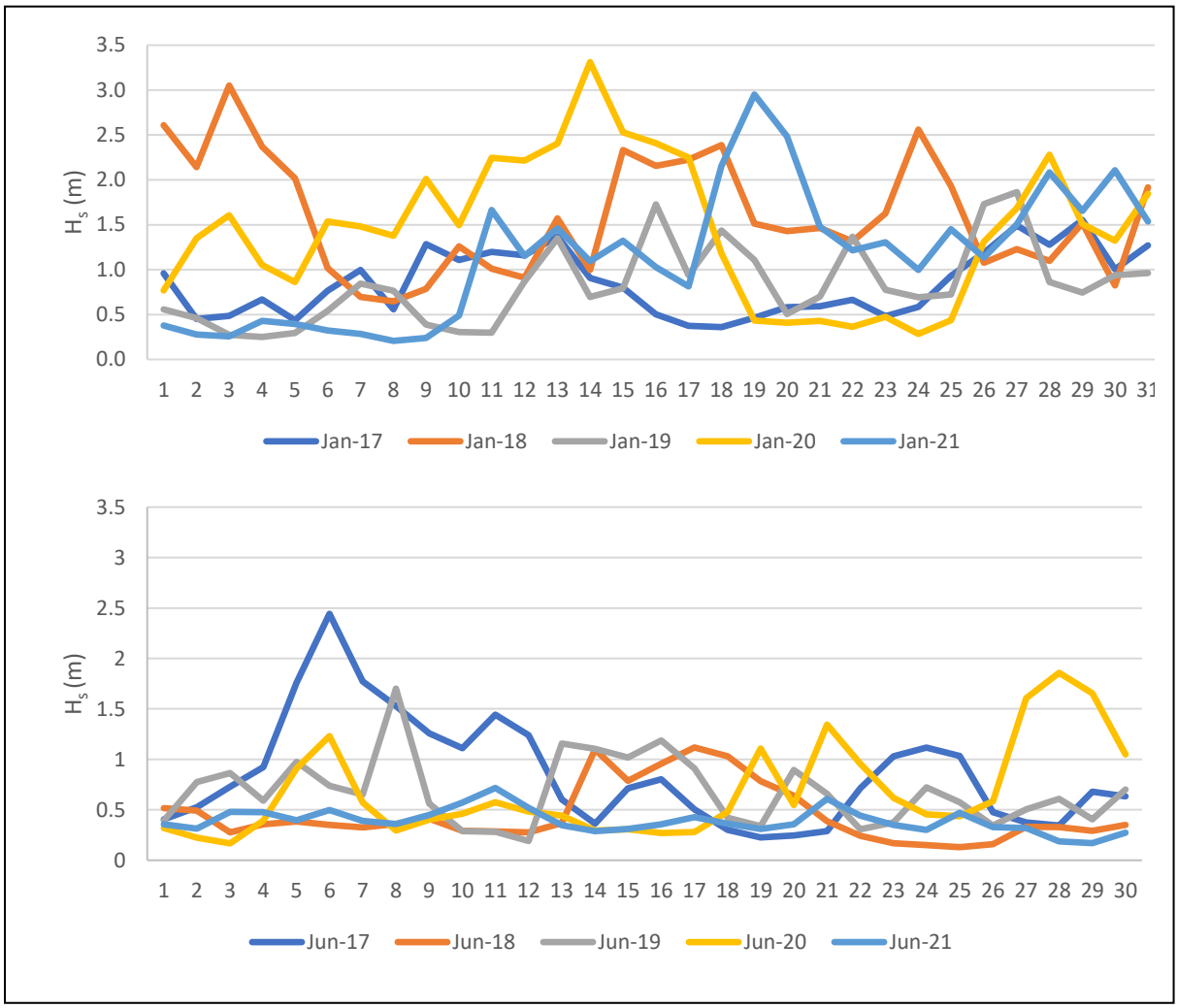

Figure 7: Daily average Significant wave height (H_S) during January (top) and June (bottom) of five consecutive years from 2017 through to 2021 for the Chesil beach/ Portland area, recorded at 30 minute intervals.

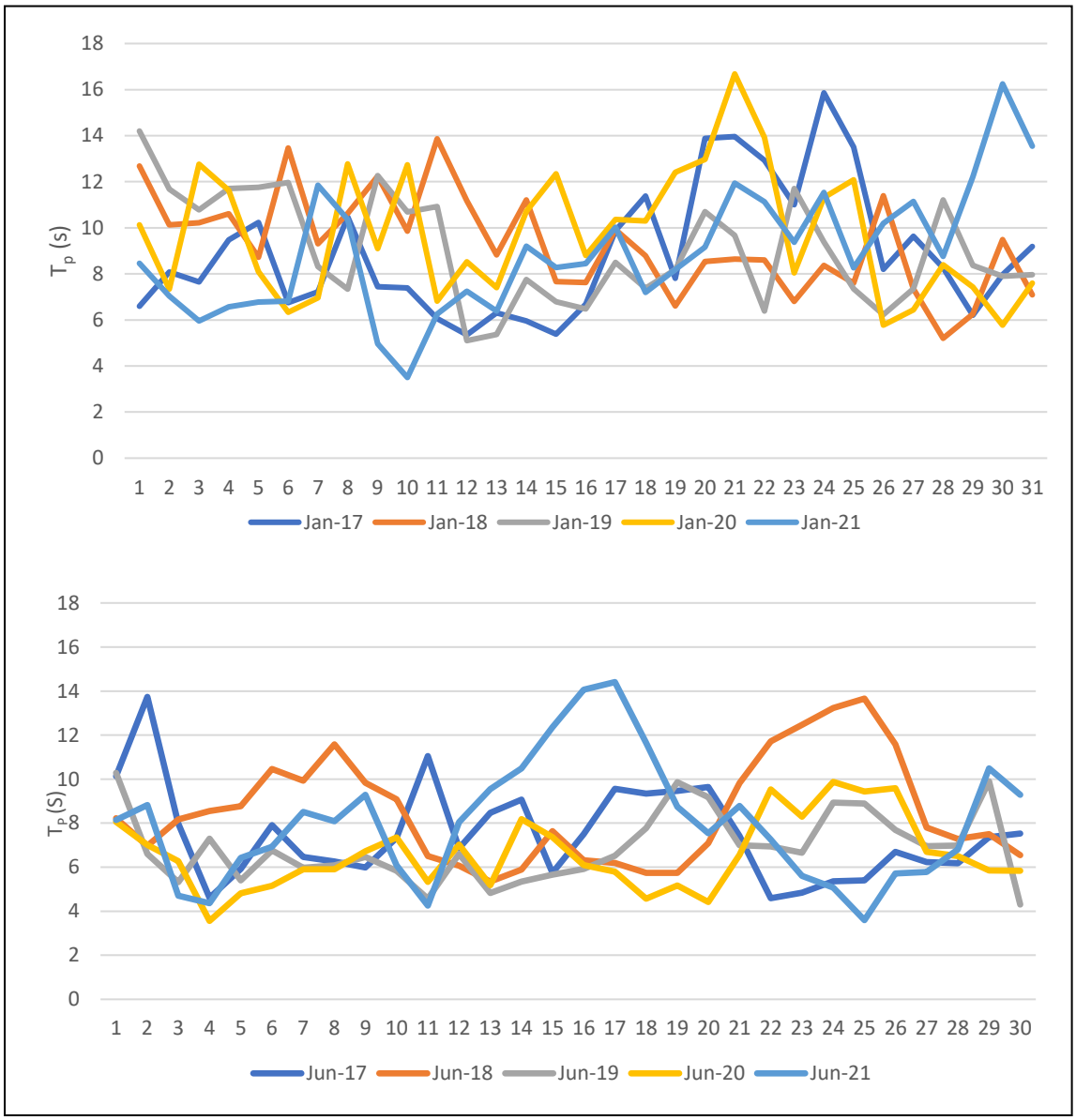

Figure 8: Daily average peak period (T_p) of five different years from 2017 through to 2021 for the Chesil beach/ Portland area recorded at 30 minute intervals for January (top) and June (bottom).

Wave Power Calculation

The hydrodynamic wave power (i.e. the power available from the waves) is given by (Silva et al., 2013) as:

$$P_W = \frac{\rho g^2}{64\pi} H_s^2 T_e,$$

where ρ = 1025 kg/m^3 is the density of sea water; g is the acceleration of gravity (9.81 m/s), and T_e is the energy period.)
Waverider buoy data typically gives values of H_s and T_p, the peak spectral period. The energy period T_e is related to the peak spectral period T_p depending on the shape of the spectrum. The typically used JONSWAP spectra represent a fetch limited sea state typical of the North

Sea in which the sea state is never fully developed (Isherwood, 1987). The JONSWAP spectrum follows the relationship:

$$T_e = \frac{T_p}{1.11},$$

A Bretschneider spectrum represents a fully developed sea state (Tucker, 1991). The Bretschneider spectrum follows $T_e = T_p / 1.17$ (Cahill and Lewis, 2014). A value of 1.11 is assumed here for a JONSWAPP case, due to similar fetch considerations.

The units of the P_w equation are in W/m, so an expression can be arrived at to give an output of power in kW/m, with inputs of T_p and H_s. This is:

$$P_W(kW/m) = \frac{\rho g^2}{1.11 \times 1000 \times 64\,\pi} H_s^2 T_p$$

This can be re written more simply using a coefficient replace the constants:

$$P_W(kW/m) = 0.44\, H_s^2 T_p$$

Figure 9 gives the wave power calculated from the wave measurements recorded at the Chesil beach (Portland) wave buoy at 30-minute intervals throughout 2021. Note the peaks throughout the year, with January recording the greatest wave power (in frequency and strength) and April, June and September the least wave power (in frequency and strength). While peaks reach almost 100 kW/m in late January, there are significant periods with very little energy. The total wave energy production over the year for this data is just under 73,000 kW/m, the average wave power calculated with the 30 minute readings throughout 2021 is 4.4 kW/m.

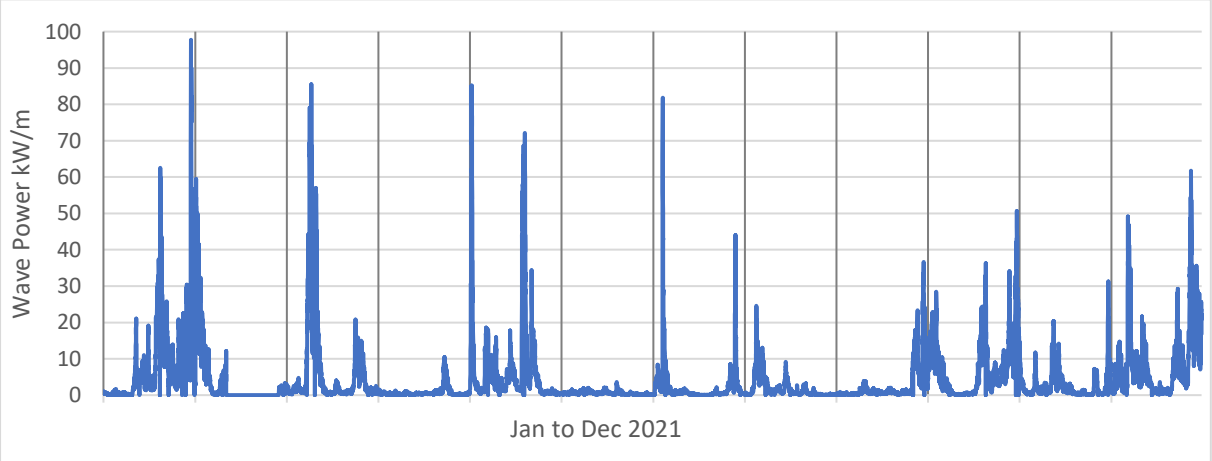

Figure 9: Wave power at the Chesil wave buoy, near Portland throughout 2021

Averaging the wave power data for multiple years reduces the influence of winter storm conditions on the time series, and gives a picture of the seasonal variability in wave power between the winter and summer months.

As with the wave height and peak period calculations, data for a representative stormy period (January) was compared with a representative calm period (June) (Figure 7 and 8) to explore the differences in winter-summer energy avaialbility. At the Chesil wave buoy, in

January 2021 the average wave power is 8 kW/m, with three spikes exceeding 20 kW/m. In June 2021 the average wave power is 2 kW/m, exceeding 4 kW/m on 6 occasions (Figure 10).

The equations above give the available wave energy and provide a convenient functional form for analysing the wave energy available, from the wave height and period. In practice, there will be a loss of energy due to conversion inefficiency, and a loss because the turbines do not operate below specific wave heights and periods.

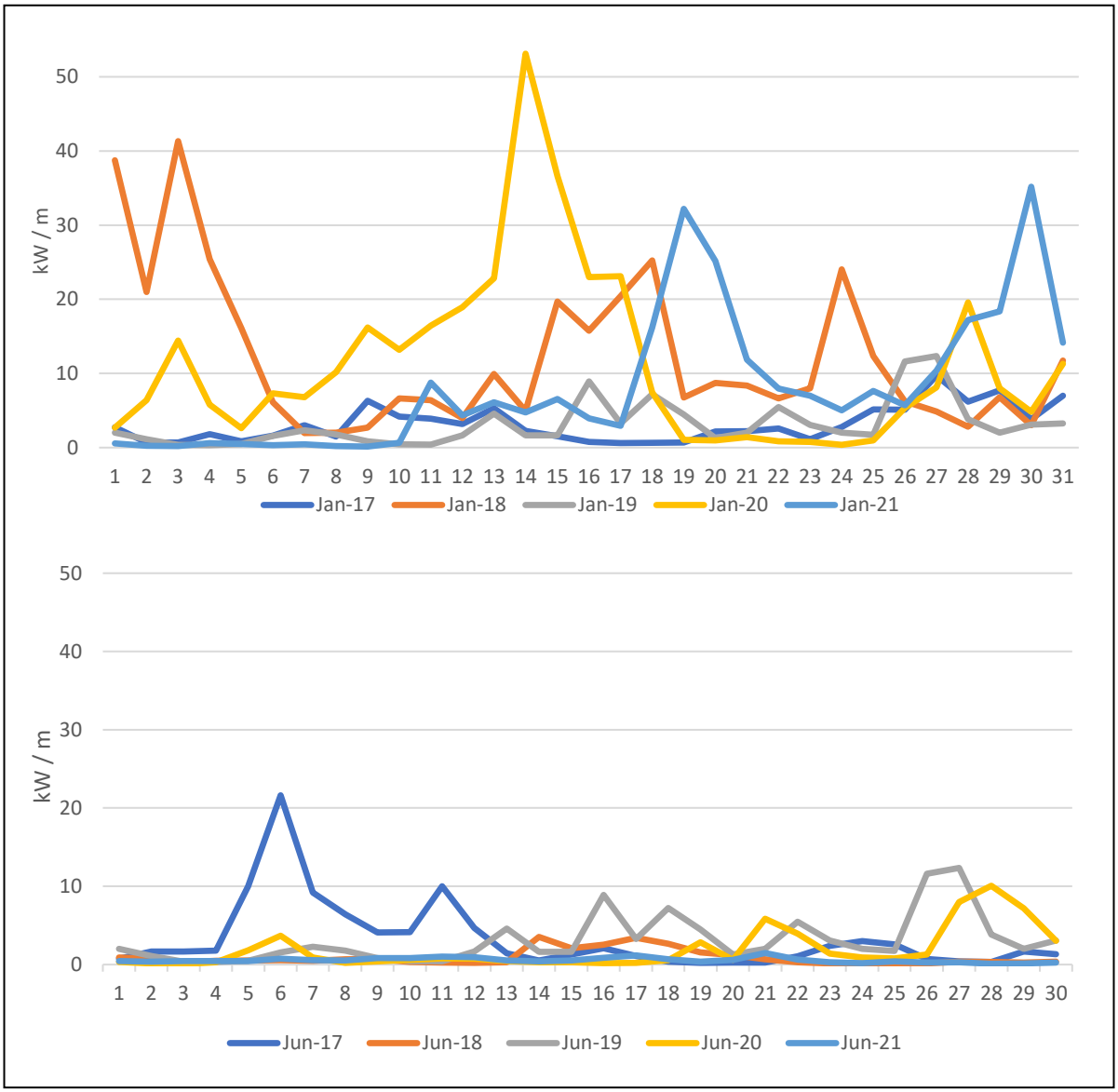

Figure 10: Daily average of wave power per meter of wave crest throughout January (top) and June (bottom) of five consecutive years. Calculated using significant wave height (Hs) and peak period (Tp) data recorded at 30 minute intervals at the Chesil beach/ Portland area.

Energy conversion efficiency

The efficiency of the device is termed the power coefficient, and is calculated as follows:

$$C_p = \frac{P_{out}}{P_w}$$

The power coefficient of the device varies depending on the wave height and period. Using the data for Oyster, and the available wave power, the power coefficient matrix is given in Table 3.

Table 3: Power coefficients for Oyster

	Oyster Power Coefficients								
Te (s) Hs (m)	**5**	**6**	**7**	**8**	**9**	**10**	**11**	**12**	**13**
0.5	0.00	0.00	0.00	0.00	0.00	0.00	0.05	0.13	0.12
1	0.50	0.63	0.68	0.66	0.61	0.55	0.49	0.49	0.44
1.5	0.89	0.79	0.73	0.68	0.63	0.58	0.53	0.47	0.45
2	0.88	0.77	0.68	0.62	0.54	0.49	0.46	0.42	0.38
2.5	0.77	0.66	0.60	0.51	0.45	0.42	0.39	0.34	0.32
3	0.67	0.55	0.47	0.42	0.38	0.32	0.30	0.27	0.25
3.5	0.00	0.46	0.40	0.35	0.31	0.27	0.25	0.22	0.21
4	0.00	0.38	0.33	0.28	0.24	0.23	0.20	0.18	0.17
4.5	0.00	0.30	0.26	0.23	0.19	0.18	0.16	0.14	0.13
5	0.00	0.00	0.21	0.18	0.16	0.14	0.13	0.12	0.11
5.5	0.00	0.00	0.17	0.15	0.13	0.12	0.10	0.10	0.09
6	0.00	0.00	0.14	0.13	0.11	0.10	0.09	0.08	0.07

It is possible to calculate an average efficiency of the device in the region relevant to the wave climate. In practice the device design would be tuned to match the environment. In this case, wave heights up to (including) 1.5 m, and across all wave periods give an average power coefficient (C_p) value of 0.41 (Other assumptions would yield other values of C_p.) Given time series of measured wave heights (H_s) and peak wave periods (T_p), the following equation can be used to calculate a time series of output power per m of wave crest:

$$P_{out}(kW/m) = 0.44\, C_p H_s^2 T_p,$$

From this time series, average wave power values and total wave power values can be ascertained.

The hydrodynamic power matrix (Table 4) shows the relationship between wave height and wave period on the power of the waves. Power of the waves increases with increased wave height and increased wave period. The values for a device efficiency matrix can be calculated by dividing the output power by the hydrodynamic power for each pair of values.

Table 4: A power Matrix generated using the hydrodynamic wave power equation

	Hydrodynamic power matrix (Formula)								
Te (s) *Hs (m)*	**5**	**6**	**7**	**8**	**9**	**10**	**11**	**12**	**13**
0.5	552	663	773	884	994	1105	1215	1326	1436
1	2210	2652	3094	3536	3978	4420	4862	5304	5746
1.5	4972	5967	6961	7956	8950	9945	10939	11934	12928
2	8840	10608	12376	14144	15912	17679	19447	21215	22983
2.5	13812	16574	19337	22099	24862	27624	30387	33149	35911
3	19889	23867	27845	31823	35801	39779	43757	47735	51712
3.5	27072	32486	37900	43315	48729	54143	59558	64972	70386
4	35359	42431	49502	56574	63646	70718	77790	84861	91933
4.5	44751	53701	62652	71602	80552	89502	98453	107403	116353

Wave power capacity over time

It is a crucial step in the analysis to get a sense of the sustained power capacity available at the site of interest. The researcher can identify periods of time where there is sustained power over and below a certain threshold for hours and days. The thresholds are determined by the operational parameters of the type of WEC being considered.
For the Portland case-study, a representative threshold was set as periods during which wave energy was between 0.17 kW/m and 18.5 kW, these are thresholds which reflect the operational parameters of the Wells turbine at the Mutriku plant. Thus, there is no power generated below a wave power value of 0.17, and there will be no additional energy generated above 18.5 kW. The OWC Wells turbines used at Mutriku have a maximum capacity of 18.5 kW, as the OWC chambers are 6 m in width, this gives a maximum capacity of 3.1 kW/m. The range of wave heights and periods that 0.17 kW/m represents is 2.5 s and 0.4 m to 20 s and 0.14 m.

Table 5: Total available wave power at Portland and the potential total generated power, based on the capabilities of the Oyster device.

2021	**Available wave Power P_w kWh/m**	**Total generated power P_o (in kW/m)**
January	5968	3640
February	6067	3700
March	717	437
April	566	345
May	5432	3313
June	403	245
July	1758	1072
August	1343	819
September	1519	927
October	5568	3396
November	1824	1113
December	6065	3700
Annual Total	**37,235**	**22,713**

For 2021, the total power for each day in each month was added up, then an average value for each month was calculated (Table 5). Using the average monthly figures of available wave power and the device efficiency reported for the Oyster, the monthly total generated power by a device such as the Oyster can be calculated. This information is useful when planning a device maintenance schedule; when considering likely import times for export to the grid, or for use with a battery storage device, or when considering creating an optimal energy generation mix within a hybrid system of tidal, wind or solar input (Coles et al., 2021).

To illustrate wave resource at the site. wave buoy data have been used to calculate a matrix of the wave energy available at Portland, from the wave climate recorded throughout 2021. Table 6 gives the sum of recorded wave data falling within the bracketed parameters of the wave height in columns and corresponding bracketed parameters of the wave period in rows.

Table 6: Calculated power matrix for available wave energy based on recorded wave climate parameters in 2021.

Total Power matrix (in kW/m)							
Te (s) Hs (m)	***.....***	**6** (5.6-6.5)	**7** (6.6-7.5)	**8** (7.6-8.5)	**9** (8.6-9.5)	**10** (9.6-10.5)	**....**
.....							
0.4 (0.3-0.49)		**179**	**181**	**224**	**158**	**345**	
0.6 (0.5-0.69)		**304**	**301**	**342**	**176**	**362**	
0.8 (0.7-0.89)		**266**	**187**	**295**	**284**	**388**	
1.0 (0.9-1.19)		**554**	**469**	**888**	**590**	**829**	
1.2 (1.2-1.39)		**767**	**393**	**611**	**307**	**624**	
.....							

Table 7 displays the number of recorded incidences and the percentage of time in which wave power at the Chesil beach wave buoy was within the working threshold of the Mutriku plant, described here as the period of exploitable power, throughout the whole of 2021 and for the month of January. As can be seen from Table 7, throughout 2021, at Portland the wave conditions for just over 90 % of the year fall above the threshold of 0.17 kW/m. During the stormy month of January, the wave energy was above the upper threshold of the exploitable power for 13 % of the time, therefore no additional power would be generated. According to the needs of a given assessment, this analysis could be repeated for a longer time series where an average across multiple years would add depth to the analysis, and, or separate analysis for each month. This type of analysis will inform the limitations of a given energy device in the location of interest and could help to inform the time of year when best to carry out any maintenance for example.

Table 7: Exploitable power recorded in the threshold above 0.17 kW/m and below 18 kW/m; the number of occurrences and percentage of time in 2021 and January.

2021 Exploitable Power*			**January 2021 Exploitable Power***		
Number of 30-minute readings > 0.17 kW/m	% of time the readings > 0.17 kW/m	% of time the readings > 18.5 kW/m	Number of 30-minute readings > 0.17	% of time readings > 0.17 kW/m	% of time the readings > 18.5 kW/m
15,155	91.5%	6%	1255	89%	13%

* Times when no data were available were omitted from total time

An additional step in a detailed study of an area would be to change the thresholds according to the operational thresholds of latest technological developments in wave energy devices or by allowing consideration of different device characteristics (e.g., from changing the orifice sizes).

Application in relation to the power requirements of the area of interest

One way to quantify the required tidal contribution is to consider the energy requirements of the area of interest for a year. For example, the population of Portland is approximately 12,797 people. In the UK, the average consumption of electrical energy per person per year is approximately 2,900 kWh (Ofgem, 2022). The Isle of Portland would currently therefore need 37,111,300 kWh per year (Miles, ICE tidal report). The number of households could also be used to inform an estimated power requirement of an area in this case, Portland has 5,175 households (Dorset Council, 2011).

The power generation characteristics of an example wave turbine are used to ascertain what size wave plant would be needed to fulfil the energy requirement of Portland given the potential wave power of the site. The length of seawall housing sufficient Oscillating Water Column (OWC) devices can be calculated using the average available wave power. Using 2021 data the available wave power is 37,235 kW h / year / m (Table 5)**.**
Available wave power (Pw) = 37,235 kWh/year/m

Cp = 0.41

Converted power (Pout) = Cp x Pw = 15,266 kWh/year/m

Converted power (Pout) in units of MWh/year/m = 15.3 MWh/year/m

Isle of Portland energy requirement = 37,111 MWh/year

Length of device needed = Energy requirement / Pout = 997 m.

If the efficiency Cp was 1, then the device length would be 37,111,000/ 15,266 = 2431 m.

Using a wall length of 2431 m, and a population of 12,797, the OWC wall length required per person is 2431/12,797 = 0.19 m/person.

Table 8: Energy demand and generation by wave turbines

	Portland Bill
Annual Island demand	37,111 MWh
Annual device power generation per m of wave	15,266 kWh/year/m
Energy structure Length	2.431 k m

To meet the energy demand of the Isle of Portland with wave energy a structure of approximately 2400 m in length would be required. The seaward side of the island is just over 10 km in length thus wave energy has the potential to be a major contributor to supplying energy for the Isle of Portland.

References

Biscay Marine Energy Platform (BiMEP): https://www.bimep.com/en/mutriku-area/technical-characteristics/

Boake, C. B., T. J.T. Whittaker, M. Folley and H. Ellen (2002). 'Overview and Initial 920 Operational Experience of the LIMPET Wave Energy Plant'. In: Proceedings of the International Offshore and Polar Engineering Conference 12. February 2015, pp. 586–594.

Cahill, B and A W Lewis (2014). 'Wave period ratios and the calculation of wave power'. In: The 2nd Marine Energy Technology Symposium, pp. 1–10.

CANDHIS: http://www.cetmef.equipement.gouv.fr/donnees/candhis/home.php.

Centre for Environment, Fisheries and Aquaculture Science (CEFAS) https://wavenet.cefas.co.uk/Map

Coles, D., Angeloudis, A., Goss, Z., and Miles, J. (2021). Tidal Stream vs. Wind Energy: The Value of Cyclic Power when Combined with Short-Term Storage in Hybrid Systems. Energie 14, 1106. https://doi.org/10.3390/en14041106

Dorset Council. Area profile for Portland (2011) https://mapping.dorsetcouncil.gov.uk/statistics-and-insights/AreaProfiles/Town/portland. Source: 2011 Census. Office for National Statistics.

Falcão, A. Wave energy utilization: A review of the technologies. In: Renewable and Sustainable Energy Reviews Volume 14, Issue 3, April 2010, Pages 899-918

Folley, M., T. Whittaker and M. Osterried (2004). 'The Oscillating Wave Surge Converter'. In: Proceedings of the International Offshore and Polar Engineering Conference January 2004, pp. 189–193. issn: 10986189

Instituto para la Diversificación y Ahorro de la Energía (IDEA) Analyses of the energy consumption of the household sector in Spain 2011. www.SECH_Spain.pdf (europa.eu)

Isherwood, R M (1987). 'Technical note: A revised parameterisation of the Jon[1]swap spectrum'. In: Applied Ocean Research 9.1, pp. 47–50. issn: 0141-1187. doi: https : / / doi . org / 10 . 1016 / 0141 - 1187(87) 90030 - url: http : / / www . sciencedirect.com/science/article/pii/0141118787900307

National Network of Regional Coastal Monitoring Programmes (NNRCMP) https://coastalmonitoring.org/

Ofgem, 2022. https://usave.co.uk/energy/how-much-energy-does-the-average-uk-household-consume/

Power-technology: Mutriku Wave Energy Plant, Basque Country, Spain (power-technology.com) June 7 2021.

Silva, D., E. Rusu and C. Guedes Soares (2013). Evaluation of Various Technologies for Wave Energy Conversion in the Portuguese Nearshore. Energies, 6, 1344-1364

Stamnes, J. (1986) Waves in Focal Regions: Propagation, Diffraction and Focusing of Light, Sound and Water Waves. https://doi.org/10.1201/9780203733998

Tucker, M J (1991). Waves in Ocean Engineering: Measurement, Analysis, Interpretation. Ellis Horwood Series in Applied Science and Industrial Techn. E. Hor[1]wood. isbn: 9780139329555. url: https://books.google.co.uk/books?id= mv5RAAAAMAAJ.

Wavenergy it: https://www.wavenergy.it/generico/the-first-worldwide-application-at-full-scale-of-the-rewec3-device-in-the-port-of-civitavecchia/2014.

Whittaker, T and Folley, M. Nearshore oscillating wave surge converters and the development of Oyster Source. In: Philosophical Transactions: Mathematical, Physical and Engineering Sciences, 28 January 2012, Vol. 370, No. 1959, The Peaks and troughs of wave energy: the dreams and the reality (28 January 2012), pp. 345-364 Published by: Royal Society Stable URL: https://www.jstor.org/stable/41348239